Electromagnetic Time Domain Modeling Using an Improved Meshless Method

Hooman Razmjoo, Masoud Movahhedi, and Ahmad Hakimi

Electrical Engineering Department, Shahid Bahonar University of Kerman, Kerman, 76169-133, Iran.
Email: Movahhedi@ieee.org

***Abstract*—In this paper, a modified meshless method, one of the meshless numerical techniques that has recently emerged in the area of computational electromagnetics, is extended to time-domain electromagnetic modeling. In the space domain, the fields at the collocation points are expanded into a series of new Shepard functions which are suggested recently and are treated with a meshless method procedure. In comparison with the most traditional schemes of the meshless methods this approximation function has lower computational cost with same level of accuracy. Application of the method for electromagnetic field computation and verification of the obtained results using theoretically known solution is also presented.**

I. Introduction

Meshless methods were developed with the objective of eliminating the mesh used in the popular finite element method (FEM). It was only after 1994, when Belytschko *et al.* proposed an extension of the finite element approach which they call the element-free Galerkin (EFG) method [1], that meshless methods became popular for engineering systems modeling. The mesh-free characteristic makes meshless methods very useful, especially for modeling discontinuities and moving boundaries where the complexity in meshing and remeshing the entire problem structure is eliminated.

There are various meshless methods as the reproducing kernel particle method (RKPM), the diffuse element method (DEM), and the partition of unity method (PUM), each one with different characteristics. One can see a revision of these methods in [2]. the Radial Basis Function (RBF) method first introduced by Kansa [3] in 1992, is a powerful interpolation technique that has become a popular meshless tool to solve partial differential equations (PDEs). A newcomer meshless method is the natural element method (NEM). This method is based on the natural neighbor concept to define the shape functions. NEM has been used with a weak form by Sukumar *et al*. [4]. In [5] a special class of PUM is used and its efficiency in electrostatic problem, Cartesian and polar coordinates, has been verified. The distinguished advantage of this method is in nonuniform node distribution domain which the shape functions are constructed according to nodes density.

Recently, a new approach to one of the biggest challenges in meshless methods, i.e. shape function construction, has been developed in [6]-[7]. According to the data fitting algorithm and PUM, a complete approach for constructing shape functions have been proposed and its performance in electrostatic and electromagnetics problems have been investigated. Interface and boundary conditions are also imposed in the proportionate treatment. It has been shown that function approximations can reach acceptable accuracy in computational electromagnetics while they save a considerable computational time.

In [8]-[9], time-domain implementation of the meshless RPIM has been investigated; while in this paper we will adopt the meshless method which has been proposed in [7] for time-domain electromagnetic problems. A 2-D electromagnetic case to verify the accuracy and efficiency of the proposed meshless method in time-domain by comparing the results of the method with that of the radial polynomial interpolation method (RPIM) is presented. We will also discuss the influence of various control parameters on the simulation results.

II. Approximation Function and its Derivatives

Most of conventional meshless methods need to compute the inversion of a matrix, which is usually an expensive process, to obtain the shape functions. In proposed procedure which has been introduced in [6]-[7] and is described in the following of the paper, there is no need to do that; and therefore, shape functions can be constructed, faster [6].

Typically, in a data fitting process, a fitting algorithm produces a function F which is of the form $F(x) = \sum_i f_i N_i(x)$ where the values f_i are the known data (e.g. function values, derivatives, etc.). Functions N_i are usually called shape functions.

One class of fitting algorithms is based on the so-called "inverse distance weighted methods" whose ancestor is Shepard's method [10]. In the basic Shepard method, scattered data (x_i, f_i) is interpolated by a function as:

$$F(x) = \frac{\sum_i f_i.w_i(x)}{\sum_i w_i(x)} \tag{1}$$

where the weights, i.e. $w_i(x)$, are typically chosen as decaying functions of the distance of x from the points x_i. The basic shape functions are thus as:

$$N_i(x) = \frac{w_i(x)}{\sum_i w_i(x)} \tag{2}$$

and the global approximation of F takes the form

$$F(x) = \sum_i f_i.N_i(x) \tag{3}$$

978-1-61284-757-3/11/$26.00 C2011 IEEE

Here, we propose a new shape function with continuity and partition of unity properties [1], which are essential provisions of any shape function, directly. This function is as the following (for one dimensional):

$$N_i(x) = \frac{\exp\left(\alpha|x - x_i|\right)}{\sum_j \exp\left(\alpha|x - x_j|\right)} \tag{4}$$

In other words, the weights of the Shepard method in the proposed approach is as:

$$w_i(x) = w(x - x_i) = \exp(\alpha\ |x - x_i|) \tag{5}$$

α is an independent positive coefficient which can change the overhang width of the shape function and its optimal setting increases the accuracy of the method. Unlike PUM, there is no need to use more than one unknown per each node to achieve acceptable accuracy.

Since, some of the shape functions, arisen from conventional meshless methods, do not satisfy the Kronecker delta property [1], imposition of the essential boundary conditions is another problem in these methods. A mixed formulation has been presented in [11] which combines Shepard shape functions for inner nodes to reduce the computational time and RPIM shape functions for boundary nodes to impose the essential boundary conditions. It is interesting to note that in the suggested shape function, by getting smaller the overhang radius of the shape function using correct set of α, the value of the shape function in the other nodes would be close to zero. So, the boundary conditions will be enforced accurately with no trouble [12].

Another advantage of the proposed shape function, unlike the shape function introduced in [5], is that its derivatives can be obtained in closed forms, simply. For one dimensional, derivatives of this function can be presented as follows:

$$\frac{\partial N_i(x)}{\partial x} = \alpha[-sign(x - x_i) + \frac{s_1}{s_0}].N_i(x) \tag{6}$$

$$\frac{\partial^2 N_i(x)}{\partial x^2} = 2\alpha\ \frac{\partial N_i(x)}{\partial x}.\frac{s_1}{s_0} \tag{7}$$

and so on; where

$$s_0 = P(x) = \sum_i w_i(x)\ , \quad s_1 = \sum_i sign(x - x_i).w_i(x) \tag{8}$$

The proposed shape function in two dimensional (2-D) is as the following:

$$\begin{aligned} N_i(x,y) &= N(x - x_i, y - y_i) \\ &= \frac{\exp\left(\alpha_x\ |x - x_i| + \alpha_y\ |y - y_i|\right)}{P(x,y)} \end{aligned} \tag{9}$$

Its derivatives would be obtained as:

$$\frac{\partial N_i(x,y)}{\partial x} = \alpha_x \left[-sign(x - x_i) + \frac{s_{1x}}{s_0}\right].N_i(x,y) \tag{10}$$

$$\frac{\partial N_i(x,y)}{\partial y} = \alpha_y \left[-sign(y - y_i) + \frac{s_{1y}}{s_0}\right].N_i(x,y) \tag{11}$$

$$\frac{\partial^2 N_i(x,y)}{\partial x^2} = 2\alpha_x\ \frac{\partial N_i(x,y)}{\partial x}.\frac{s_{1x}}{s_0} \tag{12}$$

$$\frac{\partial^2 N_i(x,y)}{\partial y^2} = 2\alpha_y\ \frac{\partial N_i(x,y)}{\partial y}.\frac{s_{1y}}{s_0} \tag{13}$$

$$\begin{aligned} \frac{\partial^2 N_i(x,y)}{\partial x \partial y} &= \alpha_x \frac{\partial N_i}{\partial y}.\frac{s_{1x}}{s_0} + \alpha_y \frac{\partial N_i}{\partial x}.\frac{s_{1y}}{s_0} \\ &+\alpha_x\alpha_y.\left[sign(x - x_i).sign(y - y_i) - \frac{s_{1xy}}{s_0}\right].N_i(x,y) \end{aligned} \tag{14}$$

and so on; where

$$\begin{aligned} s_0 &= P(x,y) = \sum_i w_i(x,y) \\ s_{1x} &= \sum_i sign(x - x_i).w_i(x,y) \\ s_{1y} &= \sum_i sign(y - y_i).w_i(x,y) \\ s_{1xy} &= \sum_i sign(x - x_i).sign(y - y_i).w_i(x,y) \end{aligned} \tag{15}$$

Moreover, the shape function and its derivatives, in three dimensional can be achieved, similarly. Here, a 2-D example is presented to illustrate the properties of the proposed shape function and its derivatives created using 25 nodes in a rectangular domain with parameters $\alpha_x = 5/d_x$ and $\alpha_y = 5/d_y$. d_x and d_y are average nodal spacing in x and y directions,

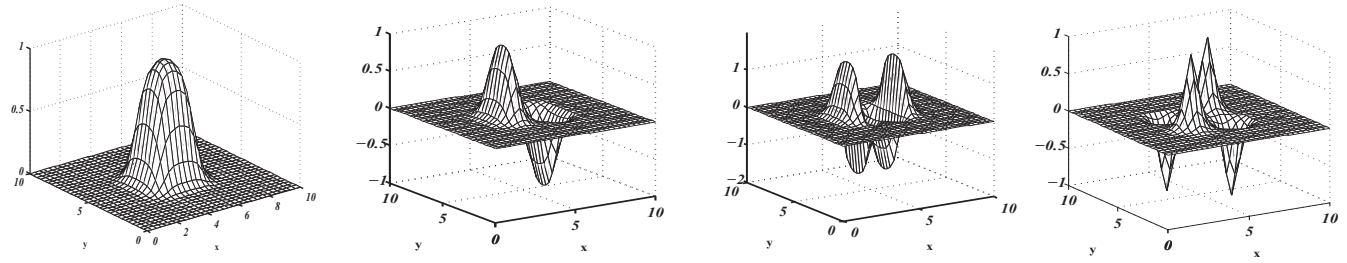

(a) (b) (c) (d)

Fig. 1. Proposed shape function and its derivatives on a (5×5) uniform node distribution for one of the middle nodes: (a) shape function ($N(x,y)$). (b) $\frac{\partial N(x,y)}{\partial x}$. (c) $\frac{\partial^2 N(x,y)}{\partial x^2}$. (d) $\frac{\partial^2 N(x,y)}{\partial x \partial y}$.

978-1-61284-757-3/11/$26.00 C2011 IEEE

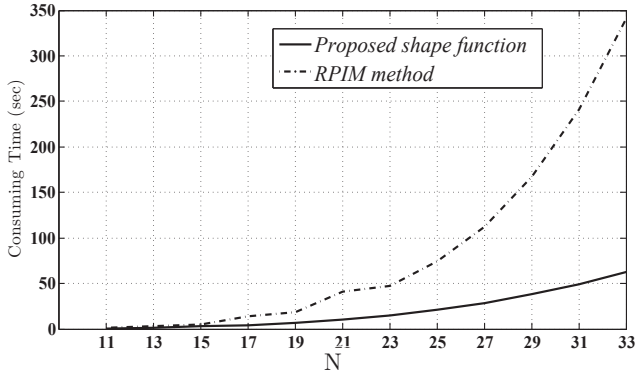

Fig. 2. Consuming time to construct the shape functions in proposed direct and RPIM-MQ methods for different number of nodes.

respectively. Figs 1(a)-(d) show the proposed shape function and its derivatives related to one of the middle nodes on an uniform (5×5) node distribution. The proposed shape functions and their derivatives possess acceptable continuity to use them for solving electromagnetic problems by the meshless methods. Simplicity of the proposed function leads to fast obtaining of all shape functions and decrease the simulation time of the meshless method. Fig. 2 illustrates the consuming time for shape function construction in two methods, proposed method and RPIM approach. As it is seen, when the number of nodes, $M(= N^2)$, increases, the RPIM method processing time increases, extremely. This is due to the computation of a $(M \times M)$ matrix inversion for its shape functions construction. But in the introduced method when the shape functions are constructed directly, there is no need to compute this matrix inversion. So, in the RPIM method, by increasing the number of nodes when the dimension of the resulted matrix is enlarged, the load of calculations would increase, extremely.

For solving electromagnetic problems in time domain, the time-dependent vector wave equation for electric field (**E**) or magnetic field (**H**) must be considered. For explanation of the proposed time-domain meshless method as a technique for solving 2-D electromagnetic problems, we consider the following scalar wave equation for TM_z wave in a homogenous medium as:

$$\frac{\partial}{\partial x}\left(\frac{1}{\mu}\frac{\partial E_z}{\partial x}\right)+\frac{\partial}{\partial y}\left(\frac{1}{\mu}\frac{\partial E_z}{\partial y}\right)+\epsilon\frac{\partial^2 E_z}{\partial t^2}=-\frac{\partial J_z}{\partial t} \quad (16)$$

To discretize (16) in time domain, a forward difference scheme on the second time-derivative is employed as:

$$\frac{\partial^2 E_z}{\partial t^2}=\frac{E_z(t+2\triangle t)-2E_z(t+\triangle t)+E_z(t)}{\triangle t^2} = \frac{E_z^{n+2}-2E_z^{n+1}+E_z^n}{\triangle t^2} \quad (17)$$

In each time step, meshless approximation would be used to discretize in space domain. So, in each time step we have

$$\frac{\partial}{\partial x}\left(\frac{1}{\mu}\frac{\partial E_z^{n+2}}{\partial x}\right)+\frac{\partial}{\partial y}\left(\frac{1}{\mu}\frac{\partial E_z^{n+2}}{\partial y}\right)+\beta E_z^{n+2}=f \quad (18)$$

where

$$\beta=\epsilon/(\Delta t^2) \quad (19)$$

$$f=\frac{J_z^{n+1}-J_z^n}{\Delta t}+\frac{2\epsilon E_z^{n+1}-\epsilon E_z^n}{\Delta t^2} \quad (20)$$

E_z^{n+2} is the unknown field function in the $(n+2)th$ time step, f and β are known parameters associated with the time discretization of the J_z and E_z.
The variational problem equivalent to boundary value problem above is given by

$$\delta F(E_z^{n+2})=0 \quad (21)$$

where

$$F(E_z^{n+2})= \frac{1}{2}\iint_\Omega\left[\frac{1}{\mu}\left(\frac{\partial E_z^{n+2}}{\partial x}\right)^2+\frac{1}{\mu}\left(\frac{\partial E_z^{n+2}}{\partial y}\right)^2+\beta\left(E_z^{n+2}\right)^2\right]d\Omega \quad (22)$$

The field function $(E_z^{n+2}(x,y))$ would be approximated in the meshless method as:

$$\tilde{E_z}^{n+2}(x,y)=\sum_{i=1}^{M}N_i(x,y).{E_z}_i^{n+2} \quad (23)$$

where ${E_z}_i^{n+2}$ are the unknown nodal function values or $E_z^{n+2}(x_i,y_i)$. To find ${E_z}_i^{n+2}$, substitute (23) into (22), take the derivative of F with respect to ${E_z}_i^{n+2}$ and it is set equal to zero. In this case, obtain

$$\frac{\partial F}{\partial {E_z}_i^{n+2}}=\sum_{j=1}^{M}{E_z}_j^{n+2}\iint_\Omega\left(\frac{1}{\mu}\frac{\partial N_i}{\partial x}\frac{\partial N_j}{\partial x}+\frac{1}{\mu}\frac{\partial N_i}{\partial y}\frac{\partial N_j}{\partial y}+\beta N_iN_j\right)d\Omega=0 \quad (24)$$

E_z^1 and E_z^2 can be obtained by initial boundary conditions.

III. Numerical Result

Here, to validate the accuracy and performance of the 2-D proposed meshless method, a simple example of the excitation of a lossless 2-D rectangular cavity in xy plane with perfectly conducting walls is studied. The dimensions of the cavity are $1.0\ cm \times 1.0\ cm$. For comparative purpose, this cavity is simulated and its dominant mode resonant frequency is obtained with both meshless methods, i.e. the proposed and a conventional (RPIM) meshless methods. The computation domain was carried out using a uniform (6×6) node distribution. On the cavity surfaces, which are assumed to be perfectly conducting walls, since the tangential components of the electric field is zero, a homogeneous Dirichlet boundary condition is imposed. The dominant mode resonant frequency can be obtained by launching a time signal and applying the Fourier transform on the time response. An excitation sinusoidally modulated Gaussian is used as current density in this simulation given by:

$$\mathbf{J}=A\cos(wt)\exp\left(-\left(\frac{t-t_0}{\tau}\right)^2\right)\hat{a}_z \quad (25)$$

978-1-61284-757-3/11/$26.00 C2011 IEEE

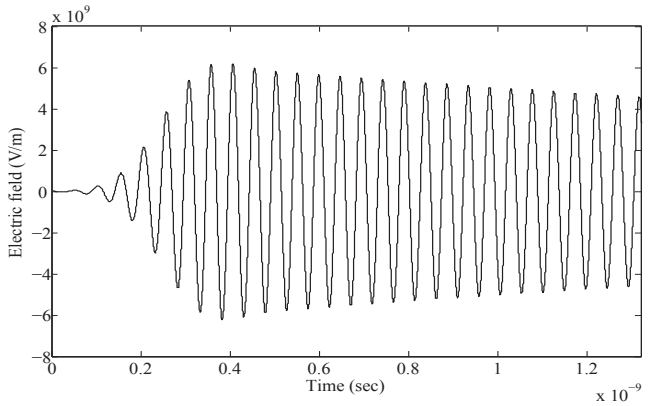

(a)

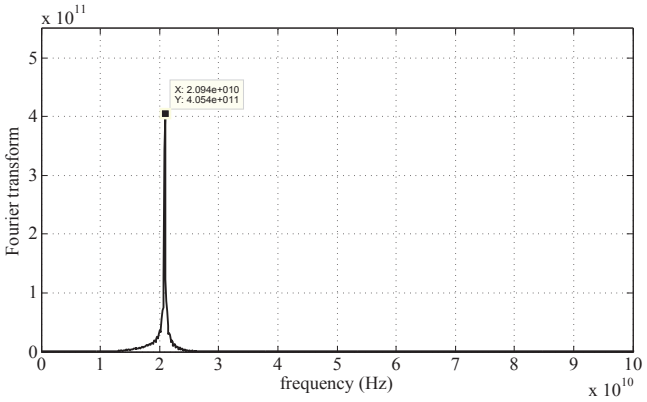

(b)

Fig. 3. Simulation results for the dominant mode in the cavity. (a) Time-domain electric fields at the center of the cavity recorded with the proposed method. (b) Fourier transform of the electric field.

where $A = 10^{10}$, $w = 2 \times \pi \times (1.9 \times 10^{10})$, $t_0 = 2.66 \times 10^{-10}$ and $\tau = 0.6 \times 10^{-10}$. The time step $\Delta t = 3.33 \times 10^{-14}$ was chosen for time discretization in both of them. Figs 3(a)-(b) present the simulation results for the dominant mode for one point within the cavity. Fig. 3(a) shows the electric field recorded at the center of the cavity and Fig. 3(b) illustrates the frequency spectrum of this signal. Resonant frequency could be seen obviously in this figure. Exact resonant frequency for this structure is 21 GHz and calculated results are 20.94 GHz and 20.93 GHz by proposed and RPIM methods, respectively. In Fig. 4, the effect of the shape parameters, i.e. α_x and α_y, in the proposed shape function on the accuracy of the proposed method is studied. It is evident from this figure that their best values are $\alpha_x = \alpha_y = \alpha \simeq 2.5/d_c$, where d_c is the average nodal spacing in x or y directions.

IV. Conclusion

A modified meshless method based on a new shape function in time domain for a 2-D electromagnetic problem has been evaluated. The main idea is using a new weight function in Shepard approximation which is formed simply. One of the advantages of the proposed shape function is its derivatives can

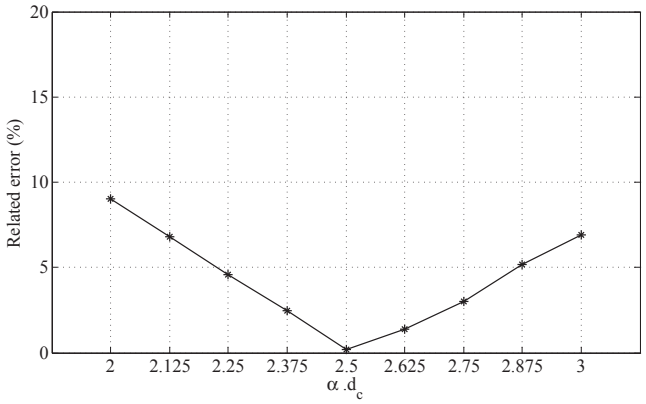

Fig. 4. Relative error versus the shape parameter α in the proposed shape function.

be calculated easily in closed forms. To impose the essential boundary condition, an efficient technique has been applied. Simulation results show that the method can reach acceptable accuracy in computational electromagnetics while it save a considerable computational time.

Acknowledgment

This work was supported in part by the Education and Research Institute for ICT of Iran (ERICT).

References

[1] T. Belytschko, Y. Y. Lu and L. Gu, "Element-free galerkin method," *Int. J. Numer. Meth. Eng.*, vol. 37, pp. 229–256, 1994.

[2] T. Belytschko, Y. Krongauz, D. Organ, M. Fleming and P. Krysl, "Meshless methods: An overview and recent developments," *Comput. Meth. Appl. Mech. Eng.*, vol. 139, pp. 3–47, May 1996.

[3] E. J. Kansa, "Multiqudrics-A scattered data approximation scheme with applications to computational fiuid-dynamics-I. Surface approximations and partial derivatives," *Comput. Math. Appl.*, vol. 19, pp. 127–145, Sep. 1992.

[4] N. Sukumar, B. Moran, A. Semenov and V. Belikov, "Natural neighbour Galerkin methods," *Int. J. Numer. Meth. Eng.*, vol. 50, pp. 1–27, 2001.

[5] H. Razmjoo, M. Movahhedi and A. Hakimi, "An efficient meshless method based on a new shape function," *Int. J. Numer. Modelling: Electronic Networks, Devices and Fileds*, vol. 23, no. 6, pp. 503–521, 2010.

[6] H. Razmjoo, M. Movahhedi, A. Hakimi, "Improved meshless method using direct shape function for computational electromagnetics," in proceedings of the *Asia-Pacific Microwave Conference (APMC 2010)*, Yokohama, Japan, Dec. 2010.

[7] H. Razmjoo, M. Movahhedi, A. Hakimi, "A modification on a fast meshless method for electromagnetic field computations," Submitted to *the IET Sci. Meas. Technol.*

[8] Y. Yu and Z. Chen, "A 3-D radial point interpolation method for meshless time-domain modeling," *IEEE Trans. Microw. Theory Tech.*, vol. 57, no. 8, pp. 2015-2020, Aug. 2009.

[9] Y. Yu and Z. Chen, "Towards the development of an unconditionally stable time-domain meshless method," *IEEE Trans. Microw. Theory Tech.*, vol. 58, no. 3, pp. 578-586, March 2009.

[10] D. Shephard, "A two-dimensional function for irregularly spaced data," in *AMC National Conf.*, pp. 517–524, 1968.

[11] A. R. Fonseca, B. C. Corra, E. J. Silva and R. C. Mesquita, "Improving the mixed formulation for meshless local Petrov-Galerkin method," *IEEE Trans. Magn.*, vol. 46, no. 8, pp. 2907–2910, Aug. 2010.

[12] C. Hkrault and Y. Markcha, "Boundary and interface conditions in meshless methods," *IEEE Trans. Magn.*, vol. 35, no. 3, pp. 1450–1453, May 1999.